

## Ring-Expansion Reactions in the Thermal Decomposition of *tert*-Butyl-1,3-cyclopentadiene

W. Sean McGivern,\* Jeffrey A. Manion, and Wing Tsang

National Institute of Standards and Technology, Physical and Chemical Properties Division, Stop 8380, Gaithersburg, Maryland 20899-8380

Received: May 31, 2006; In Final Form: September 7, 2006

The thermal decomposition of *tert*-butyl-1,3-cyclopentadiene has been investigated in single-pulse shock-tube studies at shock pressures of 182–260 kPa and temperatures of 996–1127 K. Isobutene (2-methylpropene), 1,3-cyclopentadiene, and toluene were observed as the major stable products in the thermolysis of dilute mixtures of the substrate in the presence of a free-radical scavenger. Hydrogen atoms were also inferred to be a primary product of the decomposition and could be quantitatively determined on the basis of products derived from the free-radical scavenger. Of particular interest is the formation of toluene, which involves the expansion of the ring from a five- to a six-membered system. The overall reaction mechanism is suggested to include isomerization of the starting material; a molecular elimination channel; and C–C bond fission reactions, with toluene formation occurring via radical intermediates formed in the latter pathway. These radical intermediates are analogous to those believed to be important in soot formation reactions occurring during combustion. Molecular and thermodynamic properties of key species were determined from G3MP2B3 quantum chemistry calculations and are reported. The temperature dependence of the product spectrum was fit with a detailed chemical kinetic model, and best-fit kinetic parameters were derived using a Nelder–Mead simplex minimization algorithm. Our mechanism and rate constants are consistent with and provide experimental support for the H-atom-assisted routes to the conversion of fulvene to benzene that have been proposed in the literature on the basis of theoretical investigations.

### Introduction

The formation of soot in combustion processes<sup>1</sup> is typically initiated by the creation of aromatic ring species. Small unsaturated radicals add to the aromatic species to form polycyclic aromatic hydrocarbons (PAHs). These PAH compounds act as building blocks for subsequent growth pathways, ultimately leading to particulate soot. An understanding of the early stages in the soot formation process is thus useful for controlling and restricting growth of large particulates in combustion exhaust.

A significant pathway for the formation of aromatic species in pyrolytic environments is via recombination of propargyl (C<sub>3</sub>H<sub>3</sub>) radicals to form benzene molecules. Recent theoretical studies by Miller and Klippenstein<sup>2,3</sup> have proposed several mechanistic pathways to the formation of benzene. Important among these is the rearrangement of fulvene, formed from propargyl radical recombination reactions, to benzene. In the absence of other radical species, this reaction occurs through multiple pathways, including those involving carbene or tricyclic benzvalene intermediates. Additional pathways for the rearrangement of fulvene to benzene in the presence of H atoms have been proposed by Melius et al.<sup>4</sup> with final energetics determined using bond-additivity-corrected fourth-order Moller–Plesset (BAC-MP4) methods. A more detailed computational study, including rates of reaction and evaluation of alternative mechanistic pathways, was performed by Dubnikova and Lifshitz.<sup>5</sup> A simplified mechanism for the formation of benzene from five-membered rings in the presence of H is shown in Figure 1. Addition of H to fulvene or loss of H from

one of the methylcyclopentadienyl adducts shown in the figure produces resonantly stabilized radicals that rapidly interconvert. Subsequent reaction of the (1,3-cyclopentadienyl)-5-methyl radical (**V** in Figure 1) produces benzene + H.

Experimentally, there have been previous attempts to study the ring-expansion reactions of methyl-(1,3-cyclopentadiene) (MeCp) at high temperatures. Ikeda et al. examined the pyrolysis of MeCp in a shock tube from 1000 to 2000 K over a pressure range of 7.8–78 kPa using laser schlieren techniques to examine the time dependence of the gas density with time-of-flight mass-spectrometric examination of products from a smaller subset of temperatures and pressures.<sup>6</sup> Qualitatively, a wide range of aromatic species was observed for shocks of 4.5% mixtures of MeCp, including benzene, toluene, styrene, indene, methylindene, dihydronaphthalene, naphthalene, and several larger species. Notably, the mass balance in that study was poor, which was attributed by those authors to the formation of soot. A later shock-tube study of lower-concentration mixtures was undertaken by Lifshitz and co-workers at temperatures ranging from 1070 to 1270 K in which the product spectrum was examined using gas chromatography with mass-spectrometric detection.<sup>7</sup> These studies were performed with 0.3% mixtures of MeCp, significantly decreasing the extent of bimolecular reactions relative to that in the conditions used by Ikeda et al. As in the previous shock-tube study, larger aromatic hydrocarbons were observed, including indene and naphthalene, and a large (105 elementary reactions) mechanism was used to model the pyrolysis. In this model, ring expansion from the five-membered ring system to a six-membered ring was assumed to occur via radical intermediates (Figure 1). The model fit the temperature-

\* To whom correspondence should be addressed. E-mail: william.mcgivern@nist.gov.

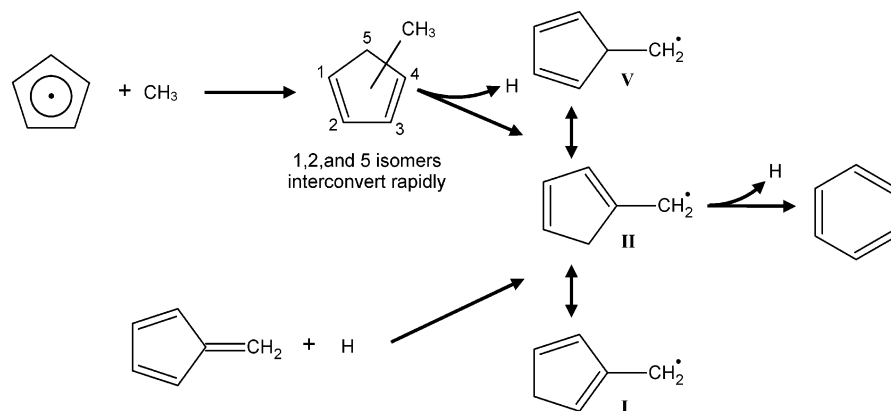
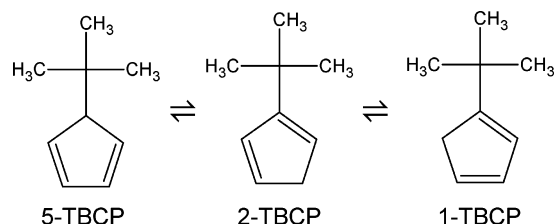


Figure 1. Ring-expansion reactions of cyclopentadienyl systems.

### SCHEME 1: Isomerization of *tert*-Butyl Cyclopentadiene



dependent data reasonably well, especially for the observed aromatic products.

The previous studies were complicated by the lack of a clean source of the intermediate believed to be responsible for the ring expansion. In particular, the ring-expansion reactions in the MeCp isomers in these previous experimental studies are likely initiated by bimolecular reactions of the reactant species with H or CH<sub>3</sub> to form RH\* (1,3-cyclopentadienyl)methyl radical isomers (I, II, and V in Figure 1). The radicals present in these studies undergo numerous reactions in addition to those involving the MeCp species. These chain processes complicate the analysis of the product spectrum and can mask some salient features of the ring-expansion reactions.

In the present study, we examine the thermal decomposition of *tert*-butyl cyclopentadiene (TBCP). The unimolecular decomposition of TBCP provides an experimentally convenient means to probe a ring expansion analogous to that shown in Figure 1 by the direct formation of radical species analogous to I, II, and V. The lack of radicals in a system initiated by unimolecular decomposition, especially when radical–radical reactions are inhibited by the presence of a radical scavenger, provides a much clearer window into the ring-expansion mechanism for these fulvene systems than the previous studies of MeCp.

TBCP exists as three isomers, which rapidly interconvert via [1,5] sigmatropic shifts of the H atom around the cyclopentadienyl ring as illustrated in Scheme 1.

In this work, the isomers are named in terms of the location of the *tert*-butyl moiety on the cyclopentadienyl ring, as shown in Scheme 1. As shown subsequently, thermal decomposition of TBCP in the temperature range of 1000–1100 K results in formation of *tert*-butyl radicals, cyclopentadienyl radicals, H atoms, methyl radicals, isobutene, cyclopentadiene, and toluene. We propose a reaction mechanism that involves the rapid isomerization of the reactant species and the radical intermediates in the system. Although the complexity, especially with regard to the initial product distribution, precludes a unique quantitative determination of many of the rate parameters, we are able to demonstrate the expansion of a five-membered ring

to a six-membered aromatic species in this system. We further establish the plausibility of the proposed mechanism by fitting the temperature dependence of the major product spectrum to a thermodynamically and kinetically self-consistent model that describes the decomposition and ring-expansion processes.

### Experiment<sup>8</sup>

Experiments were performed in a heated single-pulse shock tube, and details of the experimental apparatus and procedures have been given previously.<sup>9,10</sup> Briefly, a shock wave is created in a sample gas mixture by bursting a diaphragm separating a low-pressure (20.0 kPa) sample mixture from a higher-pressure driver gas (130–320 kPa H<sub>2</sub>). The shock wave passes through the sample gas, resulting in a substantial temperature and pressure increase behind the shock front. Subsequent interaction with the rarefaction wave results in cooling of the gas back to the initial temperature. In this apparatus, the heating is equivalent to a 500- $\mu$ s pulse heater.

Temperatures were determined using an internal standard reaction. The decomposition of *n*-propyl acetate to form propene and acetic acid was used as a reference with an Arrhenius expression of<sup>11</sup>  $\log k = 12.4 - 24000/T$ . Product distributions were determined using gas chromatography coupled with simultaneous flame ionization detection and mass spectrometry (Agilent 6890N, 5873inert with capillary splitter).

All studies were performed on dilute mixtures of TBCP, the temperature standard *n*-propyl acetate, and a free-radical scavenger (mesitylene), in a bath gas of argon (99.999%, Praxair). Samples of TBCP (a mixture of isomers) were obtained from Aldrich. Mixtures prepared by direct injection of the unpurified liquid TBCP into the sample bulb were found by GC/MS analysis to contain significant gas-phase concentrations of TBCP dimers. The presence of these species significantly affected product distributions, and results from these studies were not used in the analysis. Sample mixtures were instead made by collecting the head gas over cold liquid samples of TBCP that had undergone several freeze–pump–thaw cycles. In this case, no dimers were observed in 100 ppm mixtures down to the detection limit of the GC.

To ensure that chain processes did not affect the product distributions, mesitylene (1,3,5-trimethylbenzene, 99%, Acros Organics) was used as a radical scavenger by addition to the sample mixtures in large excess. Mesitylene reacts with hydrogen atoms to form either H<sub>2</sub> + 3,5-dimethylbenzyl radicals or *m*-xylene + methyl radicals. This latter reaction is the only source of *m*-xylene in this system, providing a means to determine H-atom concentrations, using the known<sup>12</sup> ratio of methyl displacement to H abstraction,  $k_d/k_a = \exp(-1086/T)$ .

**TABLE 1: Sample Mixtures Used in the Present Study**

component	concentration	units <sup>a</sup>
Mixture A		
TBCP isomers	100	ppm
propyl acetate	100	ppm
mesitylene	0.44	%
Mixture B		
TBCP isomers	100	ppm
propyl acetate	100	ppm
mesitylene	1.10	%

<sup>a</sup> ppm = parts per million, mole %.

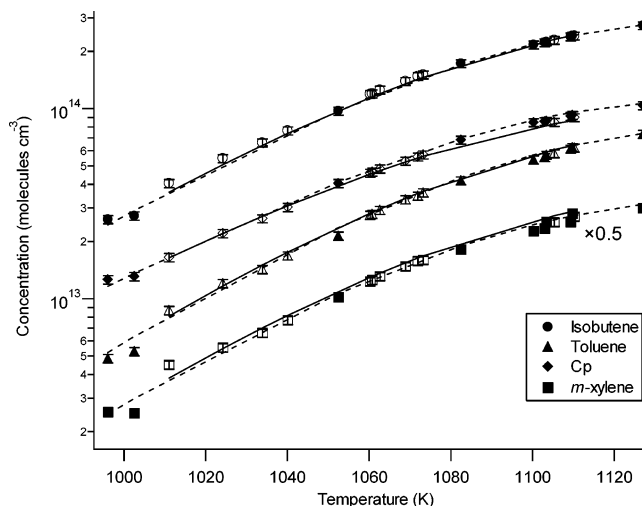
Methyl radicals can also abstract hydrogen from mesitylene to form  $\text{CH}_4$  + 3,5-dimethylbenzyl radicals. The resonantly stabilized dimethylbenzyl radicals do not undergo significant further reaction during the heating pulse, effectively preventing H and  $\text{CH}_3$  radicals from reacting with the reactant or reference species. A summary of the mixtures utilized in the present study is given in Table 1.

## Results

Major products observed from the decomposition of the mixture of TBCP isomers were isobutene (2-methylpropene), 1,3-cyclopentadiene, toluene, and H atoms, the last of which was inferred from the formation of *m*-xylene. Additional minor products were observed that are the result of various recombinations involving 3,5-dimethyl-1-benzyl ( $\text{C}_9\text{H}_{11}$ ) and cyclopentadienyl ( $\text{C}_5\text{H}_5$ ) radicals. Two distinct  $\text{C}_{10}\text{H}_{10}$  isomers were observed, although no definitive structural identification was made. Also found were a  $\text{C}_{14}\text{H}_{16}$  compound, assigned to the recombination of the dimethylbenzyl and cyclopentadienyl radicals, and a  $\text{C}_{18}\text{H}_{22}$  species from the recombination of the dimethylbenzyl radicals. No naphthalene was observed. Further experiments on the recombination products are underway and will be the subject of a future publication. Presently, we focus on the origins of the isobutene, 1,3-cyclopentadiene, toluene, and H, which are all derived from decomposition of the TBCP isomeric mixture.

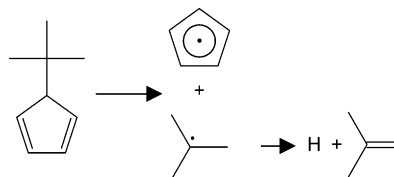
Relative concentrations of the reaction products derived from decomposition are shown as a function of temperature in Figure 2. Circles, triangles, diamonds, and squares represent the concentrations of isobutene, toluene, 1,3-cyclopentadiene, and *m*-xylene (indicative of H atoms), respectively. The concentrations of *m*-xylene have been scaled by a factor of 0.5 for separation from the 1,3-cyclopentadiene curves. The closed symbols represent runs using mixture A (Table 1), and open symbols are runs with mixture B. Error bounds were determined by parametrizing measured standard deviations from repeated runs of mixtures containing compounds over a range of different concentrations. The reported error bars represent random errors in the concentration measurements to two standard deviations and do not include possible systematic errors. The lines represent the results of a simultaneous fit using a kinetics model described below. The solid and dashed lines represent fits to data derived from mixtures B and A, respectively. The solid lines thus correspond to fits to the open symbols and the dashed lines fits to the closed symbols.

The TBCP isomer mixture undergoes several competing reactions at the temperatures of the present study. These are discussed in turn, with an emphasis on the origins of the observed products. A radical product channel, shown in Scheme 2 for the decomposition of 5-TBCP, results in the formation of cyclopentadienyl and *tert*-butyl radicals. Under these experimental conditions, the *tert*-butyl radical rapidly decomposes to

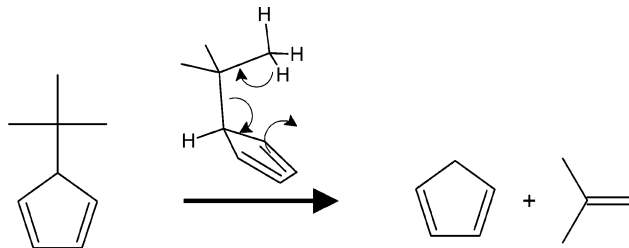


**Figure 2.** Relative concentration data for major products in the decomposition of TBCP. Circles, triangles, diamonds, and squares represent the concentrations of isobutene, toluene, 1,3-cyclopentadiene (Cp), and *m*-xylene (indicative of H atoms). The concentrations of *m*-xylene have been scaled by 0.5 for clarity. Closed and open symbols are for mixtures A and B, respectively. Dashed and solid lines show the fits of the final model to the data from mixtures A and B, respectively. Error bars are  $2\sigma$  uncertainties derived from a parametrization of estimated random measurement errors vs peak area in the GC analyses (see text).

### SCHEME 2: Bond Scission in 5-TBCP

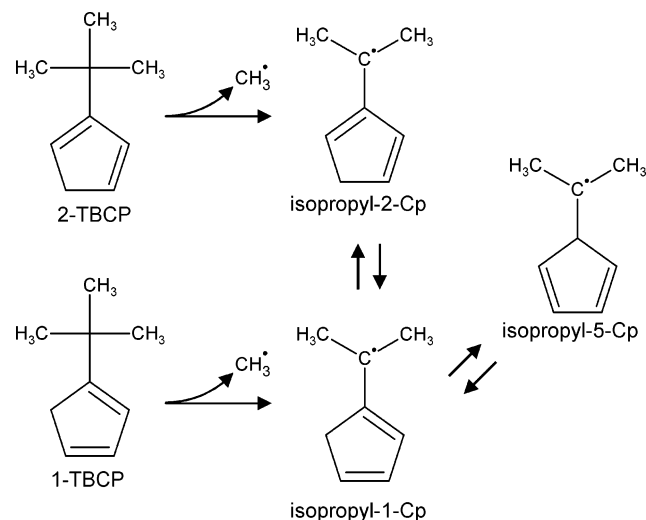
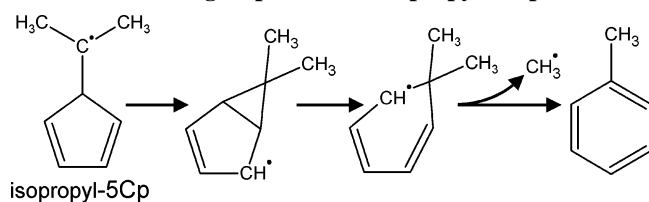


### SCHEME 3: Retro-ene Reaction in 5-TBCP



form H and isobutene.<sup>13</sup> Similar cracking of the ring-*tert*-butyl bond is expected to occur for 1-TBCP and 2-TBCP, although these reactions are energetically less favorable because they involve fission of a vinylic C–C bond.<sup>4</sup> Our data do not permit us to distinguish the reactive isomer(s), as any vinylic  $\text{C}_5\text{H}_5$  radicals formed from 1-TBCP and 2-TBCP are expected to rapidly isomerize to cyclopentadienyl radicals. The resonantly stabilized cyclopentadienyl radicals are generally unreactive toward other molecules in the system, although as discussed above, products of both self-recombination and recombination with 3,5-dimethyl-1-benzyl radicals were observed. Cyclopentadienyl radicals can also combine with H atoms in the system to form 1,3-cyclopentadiene.

A molecular pathway to isobutene and cyclopentadiene is present and occurs via a retro-ene reaction, as shown in Scheme 3. Unlike the bond scission, this reaction does not occur in 1-TBCP or 2-TBCP because no six-membered transition state for the hydrogen-atom transfer is present.

**SCHEME 4: CH<sub>3</sub>-Loss Channels and Subsequent Isomerization of 1-TBCP and 2-TBCP**

**SCHEME 5: Ring Expansion of Isopropyl-5-Cp Radical**


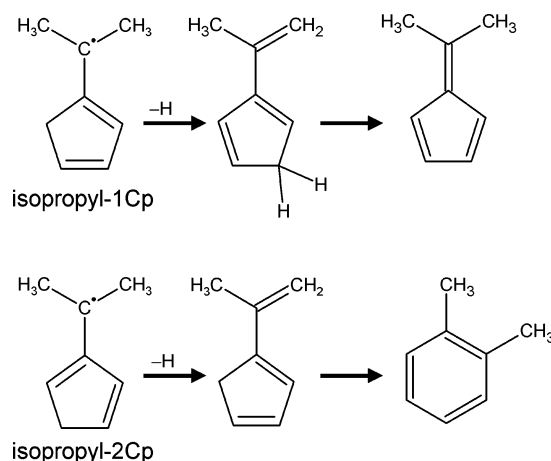
Schemes 2 and 3 provide the origins of the 1,3-cyclopentadiene, isobutene, and H-atom products; however, the ring-expansion reactions that result in the formation of toluene are more complex. The proposed mechanism for the ring expansion closely follows that proposed by Melius et al. for the H-assisted rearrangement of fulvene to benzene.<sup>4</sup> As shown in Scheme 4, the initial step in the ring-expansion mechanism is suggested to be CH<sub>3</sub> bond fission in 1-TBCP and 2-TBCP to form resonantly stabilized radicals, identified as isopropyl-1-Cp and isopropyl-2-Cp radicals for the remainder of this work. Facile H migration in the Cp ring leads to formation of all three possible isopropyl-Cp isomers, including isopropyl-5-Cp. This latter species is proposed to be the key intermediate in the ring expansion. Note that 1-TBCP and 2-TBCP are the primary sources of isopropyl-Cp radicals, because methyl loss in 5-TBCP does not lead to a resonantly stabilized product and is therefore a much higher energy process. The energetics of these processes and resulting distributions are further discussed below.

Whereas isopropyl-1-Cp and isopropyl-2-Cp radicals are more stable than isopropyl-5-Cp, the former have no obvious pathways to major product formation, whereas the latter undergoes a further fast reaction (see Scheme 5). The bicyclic cyclopropyl structure proposed therein is formed by an internal radical addition to one of the double bonds and is similar to that postulated by Melius et al.<sup>4</sup> in the decomposition of the analogous (1,3-cyclopentadienyl)-5-methyl radical.

The isopropyl-1-Cp and isopropyl-2-Cp radicals can undergo additional H-loss reactions to form conjugated trienes (Scheme 6). These species can subsequently rearrange to form dimethylfulvene and *o*-xylene from isopropyl-1-Cp and isopropyl-2-Cp radicals, respectively. Minor quantities (less than 2% of reaction) of both products were observed.

**Discussion**

The plausibility of the above mechanism was evaluated by fitting the measured product spectra using a kinetics model that

**SCHEME 6: Alkene Formation and Subsequent Rearrangement from Isopropyl-1-Cp and Isopropyl-2-Cp Radicals**

**TABLE 2: Arrhenius Parameters Used in Fitting Procedure for Reactions That Were Not Allowed to Vary**

no.	reaction	$A^b$	$E_a$ (kJ mol <sup>-1</sup> )	ref
1	TBCP-1 → TBCP-5	$1.68 \times 10^{12}$	97.4	this work
2	TBCP-5 → TBCP-1	$2.00 \times 10^{12}$	85.4	this work
3	TBCP-2 → TBCP-1	$1.03 \times 10^{12}$	86.5	this work
4	TBCP-1 → TBCP-2	$2.00 \times 10^{12}$	85.4	this work
5	isopropyl-5-Cp → toluene + CH <sub>3</sub>	$2.00 \times 10^{13}$	62.8	this work
6	<i>t</i> -butyl → isobutene + H	$8.30 \times 10^{13}$	159.6	13
7	<i>t</i> -butyl → propene + CH <sub>3</sub>	$9.96 \times 10^{12}$	172.4	17
8	H + mesitylene → 3,5- dimethyl-1-benzyl + H <sub>2</sub>	$6.56 \times 10^{-10c}$	36.1	12
9	H + mesitylene → <i>m</i> -xylene + CH <sub>3</sub>	$1.11 \times 10^{-10c}$	27.1	12
10	H + <i>c</i> -C <sub>5</sub> H <sub>5</sub> → <i>c</i> -C <sub>5</sub> H <sub>6</sub>	$4.32 \times 10^{-10c}$	0.0	18

<sup>a</sup> Values were taken from the literature or are justified in the text.

<sup>b</sup> Reported A factors are in s<sup>-1</sup> unless otherwise noted. <sup>c</sup> Units of cm<sup>3</sup> molecule<sup>-1</sup> s<sup>-1</sup>.

includes all of the reactions presented in Schemes 1–6. The reactions of primary interest are those that result in the formation of the products with concentrations shown in Figure 2. Additional bimolecular reactions were included to account for reactions of the radical scavenger as well as that of cyclopentadienyl radicals with H. Tables 2 and 3 show the reactions used in the kinetics model. Because of the large number of isomers of both the reactants and the reactive intermediates expected in this system, we employed a series of constraints to the rate constants in the kinetics model, and the implications and validity of these constraints are discussed below.

The set of differential equations resulting from this kinetics model was solved using the ODEPACK suite of differential equation solvers implemented through a Python interface.<sup>14,15</sup> Product concentrations for all of the major products (those shown in Figure 2) were calculated as a function of temperature and radical inhibitor concentration and compared to the data. A Nelder–Mead simplex algorithm<sup>15,16</sup> was utilized to determine the best-fit parameters, which are reported in Table 3. The figure of merit in the simplex minimization was the sum of the  $\chi^2$  values of the fits relative to the four major product channels and both mesitylene concentrations, as shown in Table 1. This provides for a simultaneous fit to all available data and should result in a robust means for determining appropriate Arrhenius parameters for the relevant reactions in the present system.

**TABLE 3: Best-Fit Arrhenius Parameters for Reactions Allowed to Vary in Fitting Procedure**

no.	reaction	A (s <sup>-1</sup> )	E <sub>a</sub> (kJ mol <sup>-1</sup> )
11	TBCP-5 → <i>c</i> -C <sub>5</sub> H <sub>6</sub> + isobutene	1.54 × 10 <sup>13</sup>	194.7
12	TBCP-5 → <i>c</i> -C <sub>5</sub> H <sub>5</sub> + <i>tert</i> -butyl	6.40 × 10 <sup>15</sup>	243.3
13	TBCP-2 → isopropyl-2-Cp + CH <sub>3</sub>	1.93 × 10 <sup>15</sup>	252.5
14	TBCP-1 → isopropyl-1-Cp + CH <sub>3</sub>	(1.93 × 10 <sup>15</sup> ) <sup>a</sup>	(277.6) <sup>b</sup>
15	isopropyl-1-Cp → toluene + CH <sub>3</sub>	<sup>*c</sup>	<sup>*c</sup>
16	isopropyl-2-Cp → propenyl-2-Cp + H	2.85 × 10 <sup>13</sup>	183.6
17	isopropyl-1-Cp → propenyl-1-Cp + H	(2.85 × 10 <sup>13</sup> ) <sup>a</sup>	(164.8) <sup>b</sup>
19	isopropyl-2-Cp → isopropyl-1-Cp	2.11 × 10 <sup>13</sup>	89.2
20	isopropyl-1-Cp → isopropyl-2-Cp	(1.73 × 10 <sup>13</sup> ) <sup>a</sup>	(72.5) <sup>b</sup>
21	isopropyl-1-Cp → isopropyl-5-Cp	7.88 × 10 <sup>13</sup>	159.1
22	isopropyl-5-Cp → isopropyl-1-Cp	(3.18 × 10 <sup>14</sup> ) <sup>a</sup>	(96.3) <sup>b</sup>

<sup>a</sup> The A factor for reactions with numbers in parentheses was fixed relative to that of the previous reaction in the table in the fitting procedure. <sup>b</sup> The activation energy for reactions with numbers in parentheses was fixed relative to that of the previous reaction in the table in the fitting procedure. <sup>c</sup> The rate constant for this reaction consistently became negligible during the fitting procedure, and it was not used in the final fits.

Rate constants that were not permitted to vary during the fitting procedure are listed in Table 2. These reactions were chosen to remain invariant either because they had well-established rate parameters or because the model required only that they be fast on the reaction time scale. Parameters for the decomposition of *tert*-butyl radical to form isobutene and H were taken from the literature review of Tsang.<sup>13</sup> The decomposition of *tert*-butyl radical to form propene and methyl radical was previously found to represent a ~3% channel in our temperature range.<sup>17</sup> The ratio of propene to isobutene derived from the decomposition of *tert*-butyl radicals,  $k_{C_3H_6}/k_{i-C_4H_8}$ , was presented in ref 17 relative to the rate of decomposition of cyclohexene to form ethene and 1,3-butadiene. We renormalized this ratio to the currently recommended<sup>9</sup> Arrhenius expression for the decomposition of cyclohexene to provide the following expression for the ratio of propene to isobutene

$$k_{C_3H_6}/k_{i-C_4H_8} = 0.120 \exp(-1535/T)$$

The reactions of H with mesitylene, including the displacement of methyl radicals from the ring and the abstraction of H from a terminal methyl group, have been studied previously in this laboratory.<sup>12</sup> The reaction of H with cyclopentadienyl radical was recently studied at 1150–1500 K using the shock tube/atomic resonance absorption spectroscopy technique and found to have a rate constant of  $4.32 \times 10^{-10} \text{ cm}^3 \text{ molecule}^{-1} \text{ s}^{-1}$  independent of temperature.<sup>18</sup> We chose to use this rate constant in the present work without change. The isomerization reactions of the reactant TBCP isomers (1–4 in Table 2) are required only to be fast and consistent with the relative thermodynamics of these species. They are discussed more fully in the following section. The rate constant for the reaction isopropyl-5-Cp → toluene + CH<sub>3</sub> will be justified subsequently, but has no effect on the results as long as it is fast.

Arrhenius parameters for the reactions shown in Table 3 were allowed to vary in the simplex minimization. Initial guesses were typically derived from thermodynamics of similar reactions that had well-established rate parameters. Constraints to the variable Arrhenius parameters were implemented and are utilized to describe isomerization reactions and reactions in which similar isomeric reactants and products are involved. These constraints are shown as parenthetical entries in the table. Because these similar isomers ultimately produce a small number of major products, we elected to constrain these fits in order to evaluate

the overall plausibility of the mechanism rather than allowing them to vary in an attempt to determine quantitative rate parameters.

**Isomerization Reactions.** The isomerization reactions of both the reactant 1-TBCP, 2-TBCP, and 5-TBCP molecules (Scheme 1) and the intermediate isopropyl-1-Cp, -2-Cp, and -5-Cp radicals (Scheme 4) have a significant effect on the final product distributions. We elected to treat the reactant species differently from the radical intermediates in the kinetic model. As discussed and justified below, the reactant species are assumed to be in equilibrium throughout the reaction, and ab initio thermodynamics calculations were used to determine the equilibrium reactant concentrations. For the intermediate radical species, the equilibrium assumption is not valid according to our model, and these Arrhenius parameters were allowed to vary in the minimization procedure subject to constraints detailed below.

**Reactant Isomers.** Isomerization of the reactant isomers is assumed to be fast on the time scale of the experiment, meaning that the distributions are thermodynamically controlled throughout the reaction. Whereas isomerization of TBCP has not been studied to our knowledge, several experimental and theoretical studies on close analogues of the reactant molecules have been reported. The isomerization of 5-H-perdeutero-1,3-cyclopentadiene was found by nuclear magnetic resonance (NMR) spectroscopy to have the Arrhenius expression<sup>19</sup>

$$k = 1.3 \times 10^{12} \exp[(-102 \pm 2) \text{ kJ mol}^{-1}/RT] \text{ s}^{-1}$$

in the temperature range 318–338 K in CCl<sub>4</sub>. In that study, the isomerization rate was found to be a factor of 0.32 lower in the gas phase at 323 K. Extrapolation to the reaction temperatures utilized in this study, although not expected to provide a quantitatively accurate rate constant, can provide some insight into the relevant isomerization rates. At 1000 K, the rate of isomerization is calculated to be  $6.1 \times 10^6 \text{ s}^{-1}$ , entailing a half-life of 0.11 μs. Similar NMR studies by McLean and Haynes of the isomerization of 5-methyl-1,3-cyclopentadiene both neat and in CCl<sub>4</sub> solutions yielded the following Arrhenius expression in the temperature range 278–313 K<sup>20</sup>

$$k = 2.9 \times 10^{11} \exp[(-85.4 \pm 1.2) \text{ kJ mol}^{-1}/RT] \text{ s}^{-1}$$

Extrapolation to 1000 K yields a reaction rate of  $1.0 \times 10^7 \text{ s}^{-1}$ . In addition, Bachrach calculated ab initio potential energy surfaces for the [1,5] sigmatropic hydrogen shift in 1,3-cyclopentadiene.<sup>21</sup> The barrier to rearrangement was found to be 110 kJ mol<sup>-1</sup> at the MP2/6-31G\*\*/HF/6-31G\* level of theory. Melius et al. calculated isomerization barriers for all of the methyl cyclopentadiene isomers using a bond-additivity-corrected MP4 (BAC-MP4) method and found that they ranged from 115 to 130 kJ mol<sup>-1</sup>.<sup>4</sup> However, they noted that the BAC-MP4-calculated [1,5] sigmatropic H-shift isomerization barriers in various cyclopentadienyl derivatives overestimated experimental values by 18–25 kJ mol<sup>-1</sup>. All of the above data are consistent with our assumption that isomerization of TBCP is fast relative to the 500-μs time scale of the shock pulse. We arbitrarily chose to use the following rate expression for both the 5 → 1 and 1 → 2 (exothermic) isomerizations

$$k = 2.0 \times 10^{11} \exp(-85.4 \text{ kJ mol}^{-1}/RT) \text{ s}^{-1}$$

The reverse reaction rate expressions were derived from calculations of thermodynamic parameters as discussed below.

**Thermodynamic Properties of 1-, 2-, and 5-TBCP.** To our knowledge, the thermodynamic properties of the TBCP isomers have not been experimentally determined. We derived these

parameters from G3MP2B3 quantum chemistry calculations<sup>22</sup> and checked our computational method by comparing the results of analogous calculations on the methylcyclopentadienes, for which experimental data are available. Calculations were performed on the Biowulf PC/Linux cluster at the National Institutes of Health in Bethesda, MD, and a Pentium 4 PC at NIST using the Gaussian 03 software package.<sup>23</sup> G3MP2B3 calculations were performed on the ground states of 1-TBCP, 2-TBCP, and 5-TBCP molecules. Thermodynamic functions were derived with the NIST ChemRate program.<sup>24,25</sup> Over our experimental temperature range, the relative entropies and enthalpies are essentially linear with respect to temperature. Hence, the equilibrium constants can be represented as ratios of simple Arrhenius rate expressions for the forward and reverse reactions. Appropriate ratios of *A* factors and differences in activation energies for the forward and backward isomerization reactions were derived for 1050 K, the approximate midpoint temperature of our studies. The resulting parameters were used to determine the constraints shown in Table 3. The frequencies and rotors used to derive the entropies and enthalpies used in the calculation of the *A* factor ratios and activation energy differences are listed in Table 4. Tables of temperature-dependent thermodynamic parameters for all species for which G3MP2B3 thermodynamics were calculated are provided as Supporting Information. The calculated G3MP2B3 thermodynamic parameters and relative equilibrium concentrations are reported in Table 5 for the reactant species at 1050 K.

To evaluate the validity of the G3MP2B3 computational method for the present system, we additionally calculated thermodynamic parameters of the 1-, 2-, and 5-methyl-1,3-cyclopentadiene (MeCp) molecules, for which experimental equilibrium data are available. These parameters were then used to calculate the expected equilibrium distribution of isomers as a function of temperature. At 239 K, McLean and Haynes found an equilibrium distribution of 0.80:1:0.02 for the 1, 2, and 5 isomers, respectively, of MeCp in liquid ammonia.<sup>20</sup> Calculation of the gas-phase equilibrium distribution from the G3MP2B3 thermodynamics at this temperature yields 0.50:1:0.0008 for 1, 2, and 5 isomers. Additional equilibrium experiments by McLean and Haynes<sup>20</sup> yielded 0.82:1 and 0.86:1 for the ratio of the 1- and 2-MeCp isomers in various solvents at room temperature. The calculated G3MP2B3 gas-phase ratio for room-temperature equilibrium is 0.59:1. The calculated values show good qualitative agreement with the experimental values, and the differences can likely be attributed to both solvent effects and experimental error. In particular, the relatively large differences between the calculated and measured equilibrium concentrations of 5-MeCp (0.0008 vs 0.02, respectively) might be due to a small amount of unreacted material present in the solution study, because 5-MeCp was used as a reactant.

Previous theoretical studies have also evaluated the relative energies of the MeCp isomers. Melius et al. found 0:0:9 kJ mol<sup>-1</sup> for the relative enthalpies of the 1-, 2-, and 5-MeCp isomers at the BAC-MP4 level.<sup>4</sup> Dubnikova and Lifshitz calculated 0.9:0:12.8 kJ mol<sup>-1</sup> for the relative energies of 1-, 2-, and 5-MeCp at the QCISD(T)/cc-pVDZ//B3LYP/cc-pVDZ level of theory. Although these calculated values are not enthalpies, corrections to the relative heats of formation are expected to be no larger than 1 kJ mol<sup>-1</sup>. Relative thermodynamics from G3MP2B3 calculations can be found in Table 5. The relative enthalpies at 298 K were found to be 1.3:0:13.5 kJ mol<sup>-1</sup> for 1-, 2-, and 5-MeCp. The good agreement between the calculated G3MP2B3 parameters and the previous experimental and theoretical work gives us confidence that the

quantum chemistry calculations on the reactant TBCP isomers provide reasonable thermodynamic parameters for the calculation of the equilibrium distributions.

*Intermediate Radical Isomers.* Unlike the closed-shell reactant species, the isomerization of the radical isomers isopropyl-1-Cp, -2-Cp, and -5-Cp cannot be treated as a simple equilibrium problem. The enthalpies of formation of the three isomers differ markedly because of allylic resonance stabilization in both the 1-Cp and 2-Cp isomers that is not present in the 5-Cp isomer. This large difference in stabilization implies that an a priori assumption that the isomers are in equilibrium is inappropriate. Dubnikova and Lifshitz calculated rate expressions for isomerization from the QCISD(T) thermochemistry. The calculated Arrhenius expression for the exoergic isomerization of the 2-(1,3-cyclopentadienyl)methyl radical to the 1-(1,3-cyclopentadienyl)methyl radical is

$$k_{\infty} = 3.7 \times 10^{13} \exp(-131.8 \text{ kJ mol}^{-1}/RT) \text{ s}^{-1}$$

which corresponds to a reaction rate of  $1.0 \times 10^7 \text{ s}^{-1}$  at 1050 K. This is similar to the isomerization rates observed for the reactants and is fast on the time scale of reaction in the present system. However, because of the large differences in relative stabilities expected for these radicals, the reverse isomerization reactions are likely comparable to the reaction time scale, and the Arrhenius parameters for these reactions were explicitly allowed to vary in the present system (Table 3).

As in the case of the reactant molecules, we fixed the ratios of the *A* factors and differences in the activation energies for the forward and reverse reactions. We attempted to utilize G3MP2B3 calculations to obtain the thermodynamics of the radical intermediates to use as constraints. The results are shown in Table 5. The allylic stabilization in isopropyl-2-Cp was found to provide 59.7 kJ mol<sup>-1</sup> of resonance energy, and the additional conjugation via the cyclopentadienyl ring in isopropyl-1-Cp provides another 21.9 kJ mol<sup>-1</sup> of stabilization. These values can be compared to previous calculations of the radical energetics in MeCp. Dubnikova and Lifshitz performed quantum chemistry calculations on 1-, 2-, and 5-(1,3-cyclopentadienyl)methyl radicals at the QCISD(T)/cc-pVDZ//B3LYP/cc-pVDZ level of theory.<sup>5</sup> As expected, the 1-(1,3-cyclopentadienyl)methyl radical isomer (analogous to isopropyl-1-Cp) was most stable, followed by the 2-(1,3-cyclopentadienyl)methyl radical. The 5-(1,3-cyclopentadienyl)methyl radical is the highest energy isomer with no allylic stabilization of the radical. Those authors calculated relative energies for the 1-, 2-, and 5-(1,3-cyclopentadienyl)methyl radicals to be 0:21.1:85.6 kJ mol<sup>-1</sup>. Melius et al. also performed quantum chemistry calculations of the methyl cyclopentadiene radical intermediates<sup>4</sup> and found relative enthalpies (298 K) of 0:27:114 kJ mol<sup>-1</sup> for the 1-, 2-, and 5-(1,3-cyclopentadienyl)methyl radical intermediates. The present G3MP2B3-calculated enthalpies of 0:21.9:81.6 kJ mol<sup>-1</sup> for the 1, 2, and 5 isomers of isopropyl-*n*Cp are similar to the QCISD(T) calculations of Dubnikova and Lifshitz for the (1,3-cyclopentadienyl)methyl radical species.

On the basis of these computational results, we attempted to fix the relative differences in activation energies to the calculated G3MP2B3 enthalpy values at 1050 K. Similarly, we fixed the ratios of Arrhenius *A* factors for the radical isomerization reactions to correspond to the calculated values of the reaction entropy change at 1050 K. The Arrhenius parameters for the isopropyl-1-Cp  $\rightarrow$  isopropyl-5-Cp and isopropyl-1-Cp  $\rightarrow$  isopropyl-2-Cp reactions were then allowed to vary during the simplex minimization. When the G3MP2B3 values were used to generate the *A*-factor and activation-energy

**TABLE 4: Molecular Properties Derived from G3MP2B3 Calculations Used for Determination of Relative Thermodynamic Parameters**

species	property	
TBCP-1	frequencies (cm <sup>-1</sup> )	143.7, 292.5, 305.1, 330.3, 343.5, 367.5, 462.4, 466.2, 555.3, 573.0, 698.5, 809.8, 820.5, 885.0, 889.5, 932.8, 938.5, 946.0, 950.5, 970.5, 971.8, 1032.1, 1055.8, 1057.3, 1107.7, 1134.3, 1152.3, 1236.4, 1236.9, 1278.3, 1298.8, 1333.3, 1399.0, 1421.6, 1425.5, 1450.3, 1453.6, 1510.7, 1516.6, 1521.0, 1532.1, 1534.5, 1548.8, 1595.4, 1671.2, 3032.5, 3038.5, 3041.9, 3049.7, 3058.1, 3103.7, 3107.2, 3114.1, 3115.3, 3118.2, 3118.6, 3209.8, 3229.0, 3240.6
	moments of inertia (amu·Å <sup>2</sup> )	external: <sup>a</sup> 493.5, 437.4 (466.0, inactive), 170.8 internal: <sup>b</sup> 38.9 (3, 6.3 kJ mol <sup>-1</sup> ), 3.1 (3, 17.2 kJ mol <sup>-1</sup> ) × 3
TBCP-2	frequencies (cm <sup>-1</sup> )	141.0, 209.1, 229.8, 328.8, 337.7, 369.2, 420.2, 464.7, 573.7, 646.6, 719.9, 781.1, 812.4, 820.1, 908.6, 935.8, 939.6, 945.6, 949.0, 951.6, 970.4, 1001.8, 1051.3, 1058.6, 1106.0, 1132.5, 1152.3, 1236.5, 1239.8, 1282.3, 1288.2, 1329.6, 1402.3, 1423.0, 1423.2, 1452.8, 1454.8, 1509.5, 1516.9, 1519.3, 1532.8, 1532.8, 1548.3, 1596.2, 1680.7, 3023.5, 3040.8, 3041.4, 3046.2, 3049.3, 3106.4, 3107.6, 3113.4, 3114.9, 3118.2, 3119.6, 3209.3, 3236.8, 3240.4
	moments of inertia (amu·Å <sup>2</sup> )	external: 492.5, 435.6 (463.2, inactive), 171.9 internal: 39.3 (3, 7.9 kJ mol <sup>-1</sup> ), 3.1 (3, 17.2 kJ mol <sup>-1</sup> ) × 3
TBCP-5	frequencies (cm <sup>-1</sup> )	128.3, 204.1, 234.5, 334.9, 357.4, 406.6, 435.3, 546.8, 564.7, 694.1, 719.5, 800.7, 812.7, 838.7, 886.0, 943.5, 944.5, 953.0, 953.5, 975.6, 990.6, 1026.2, 1026.3, 1057.1, 1078.3, 1131.0, 1142.2, 1194.2, 1225.3, 1270.0, 1276.7, 1314.3, 1332.0, 1422.7, 1428.5, 1430.3, 1459.1, 1511.4, 1518.4, 1518.8, 1534.0, 1538.8, 1548.0, 1576.3, 1662.6, 2973.8, 3039.1, 3042.7, 3050.6, 3099.7, 3105.1, 3111.8, 3117.1, 3120.0, 3125.7, 3207.3, 3218.8, 3240.2, 3245.2
	moments of inertia (amu·Å <sup>2</sup> )	external: 457.9, 404.0 (430.1, inactive), 176.0 internal: 48.1 (3, 23.8 kJ mol <sup>-1</sup> ), 3.1 (3, 17.2 kJ mol <sup>-1</sup> ) × 3
isopropyl-1-Cp	frequencies (cm <sup>-1</sup> )	165.0, 226.1, 330.5, 351.5, 448.4, 476.5, 550.1, 555.5, 655.7, 760.8, 810.0, 825.7, 929.1, 933.2, 949.4, 970.5, 979.0, 993.7, 1063.0, 1092.5, 1120.3, 1137.6, 1161.3, 1190.1, 1289.1, 1297.7, 1339.9, 1412.0, 1438.5, 1447.3, 1474.0, 1500.6, 1502.4, 1514.7, 1517.9, 1535.4, 1600.3, 3010.6, 3017.9, 3022.2, 3044.6, 3046.9, 3051.9, 3137.5, 3143.7, 3209.3, 3233.4, 3242.3
	moments of inertia (amu·Å <sup>2</sup> )	external: 453.4, 342.7 (394.2, inactive), 120.0 internal: 30.0 (2, 62.7 kJ mol <sup>-1</sup> ), 3.1 (3) × 2
isopropyl-2-Cp	frequencies (cm <sup>-1</sup> )	172.2, 239.7, 339.2, 358.9, 402.8, 469.0, 555.8, 581.7, 629.8, 751.1, 792.5, 859.9, 930.5, 943.0, 950.9, 964.3, 975.6, 986.8, 1010.0, 1080.1, 1109.5, 1130.8, 1152.4, 1199.1, 1288.6, 1307.5, 1364.3, 1412.4, 1435.6, 1448.1, 1467.9, 1478.3, 1497.5, 1513.6, 1514.5, 1555.4, 1651.6, 2996.0, 3006.0, 3008.9, 3013.6, 3039.2, 3045.3, 3144.5, 3145.1, 3215.1, 3237.4, 3240.1
	moments of inertia (amu·Å <sup>2</sup> )	external: 458.3, 348.2 (399.5, inactive), 119.4 internal: 29.8 (2, 46.0 kJ mol <sup>-1</sup> ), 3.1 (3) × 2
isopropyl-5-Cp	frequencies (cm <sup>-1</sup> )	122.5, 177.7, 332.2, 334.9, 368.9, 525.9, 562.3, 706.1, 725.4, 805.8, 833.7, 844.2, 913.4, 948.6, 954.3, 960.9, 992.7, 1007.9, 1012.9, 1038.0, 1066.7, 1122.3, 1134.7, 1183.1, 1217.7, 1298.9, 1320.0, 1339.3, 1414.1, 1428.1, 1444.8, 1498.7, 1506.7, 1511.1, 1525.0, 1570.0, 1658.3, 2948.7, 2971.5, 2993.8, 3041.6, 3047.9, 3094.8, 3120.1, 3206.2, 3217.2, 3236.6, 3242.3
	moments of inertia (amu·Å <sup>2</sup> )	external: 371.6, 355.9 (363.7, inactive), 126.1 internal: 35.4 (2), 3.1 (3) × 2
1-methyl-Cp	frequencies (cm <sup>-1</sup> )	150.6, 229.0, 370.4, 525.1, 616.6, 693.2, 818.6, 854.7, 882.0, 929.7, 950.1, 958.2, 1007.0, 1037.6, 1063.1, 1134.3, 1152.1, 1200.5, 1281.3, 1332.6, 1402.1, 1443.3, 1450.3, 1509.5, 1518.7, 1604.4, 1685.8, 3022.2, 3027.9, 3049.2, 3067.2, 3116.1, 3205.2, 3217.9, 3240.8
	moments of inertia (amu·Å <sup>2</sup> )	external: 213.8, 157.1 (183.2, inactive), 63.0 internal: 3.0 (3, 5.9 kJ mol <sup>-1</sup> )
2-methyl-Cp	frequencies (cm <sup>-1</sup> )	158.1, 233.2, 369.0, 577.4, 617.7, 706.8, 753.8, 819.6, 915.0, 936.4, 943.2, 949.8, 983.7, 1029.5, 1081.0, 1118.4, 1132.9, 1222.1, 1279.1, 1310.2, 1406.9, 1443.5, 1453.4, 1511.1, 1521.6, 1599.3, 1697.0, 3024.5, 3034.0, 3047.3, 3080.2, 3122.6, 3204.7, 3223.6, 3236.7
	moments of inertia (amu·Å <sup>2</sup> )	external: 214.0, 156.3 (182.9, inactive), 63.9 internal: 3.0 (3, 6.3 kJ mol <sup>-1</sup> )
5-methyl-Cp	frequencies (cm <sup>-1</sup> )	167.6, 293.1, 542.1, 561.6, 717.3, 721.0, 785.3, 809.7, 874.4, 950.9, 952.8, 960.0, 1004.4, 1031.6, 1088.1, 1104.4, 1124.4, 1152.9, 1278.0, 1300.0, 1332.9, 1417.2, 1438.2, 1530.0, 1530.1, 1577.6, 1663.2, 2994.2, 3050.6, 3115.4, 3128.8, 3205.8, 3215.1, 3231.5, 3238.8
	moments of inertia (amu·Å <sup>2</sup> )	external: 193.6, 142.9 (166.3, inactive), 72.2 internal: 3.0 (3, 16.3 kJ mol <sup>-1</sup> )

<sup>a</sup> The molecules were treated as symmetric tops with the moment of inertia around the nonunique axes taken to be the geometric mean of the two largest moments of inertia in the molecule. This value is shown in parentheses. The moment of inertia about the unique axis of the symmetric top was taken to be the smallest molecular moment of inertia. <sup>b</sup> The symmetry number of the internal rotor is shown in parentheses. If a hindered rotor was used to model the rotation, the barrier to hindrance is given in kJ mol<sup>-1</sup>. Multiple identical rotors (such as the methyl rotors in the TBCP isomers) are denoted by ×*n* after the given moment of inertia, where *n* is the number of rotors.

constraints, the model was unable to reproduce the measured toluene concentrations for any reasonable values of the remain-

ing Arrhenius parameters. Therefore, we assumed that the G3MP2B3 calculations overestimated the relative enthalpies for

TABLE 5: Summary of Thermodynamic Parameters Derived from G3MP2B3 Calculations

species	relative $\Delta_f H(298\text{ K})$ (kJ mol <sup>-1</sup> )	entropy (298 K) (J mol <sup>-1</sup> K <sup>-1</sup> )	relative $\Delta_f H(1050\text{ K})$ (kJ mol <sup>-1</sup> )	entropy (1050 K) (J mol <sup>-1</sup> K <sup>-1</sup> )	relative equilibrium concentrations at 1050 K
1-TBCP	2.06	394.7	1.12	753.4	0.44
2-TBCP	0	398.6	0	759.1	1
5-TBCP	11.06	391.5	13.16	754.9	0.13
isopropyl-1-Cp	0	401.7	0	694.1	1
isopropyl-2-Cp	21.93	402.7	22.36	695.8	0.095
isopropyl-5-Cp	81.61	419.4	78.23	706.2	0.00055
1-methyl-Cp	1.57	320.1	1.34	533.9	0.90
2-methyl-Cp	0	319.3	0	533.4	1
5-methyl-Cp	11.90	309.7	13.46	526.1	0.089

the radical isomer species. We instead elected to use an approximate value of 46.1 kJ mol<sup>-1</sup> for the resonance energy of the allylic radical moiety in the isopropyl-1-Cp and isopropyl-2-Cp isomers. This energy should represent a good estimate of the relative energy difference between the isopropyl-2-Cp and isopropyl-5-Cp isomers. The additional resonance energy gained from the addition of a second conjugated double bond in the cyclopentadienyl ring, as is found in isopropyl-1-Cp but is absent in isopropyl-2-Cp, was assumed to be approximately 16.7 kJ mol<sup>-1</sup>. The relative enthalpies of the isopropyl-*n*-Cp radical isomers were thus chosen to be 1:2:5 = 0:16.7:62.8 kJ mol<sup>-1</sup>. Using these values, we obtained a good fit to all of the measured concentrations; the final values for the varied Arrhenius parameters are reported in Table 3.

**Other Reactions.** In the decomposition of the methyl-1,3-cyclopentadiene molecules, Dubnikova and Lifshitz proposed pathways for “direct” ring expansion from (1,3-cyclopentadienyl)-1-methyl and (1,3-cyclopentadienyl)-2-methyl radicals to cyclohexadienyl radical. One set of pathways involves a carbene intermediate, whereas the other set undergoes ring-opening of the cyclopentadienyl ring.<sup>5</sup> These two pathways were calculated to proceed in parallel. However, in their study, the calculated overall rate of the “direct” expansion of these two isomers, despite the vastly larger concentrations of the 1 and 2 isomers than of the 5 isomer, was dwarfed by the calculated rate of ring-opening via the (1,3-cyclopentadienyl)-5-methyl radical. In the TBCP system, the analogous reactions would be of the isopropyl-1-Cp and isopropyl-2-Cp radicals forming toluene and methyl radicals directly. We attempted to incorporate these reactions into the model by providing a direct pathway for the formation of toluene from isopropyl-1-Cp. However, irrespective of the initial guess, the Arrhenius parameters in the simplex minimization consistently produced negligible reaction rates, suggesting that these pathways are unimportant. This is indicated in Table 3 by asterisked entries.

The molecular elimination channel for the TBCP-5 isomer (Scheme 3 and Table 3) occurs via a retro-ene reaction involving the transfer of a terminal methyl H atom to the cyclopentadienyl moiety. The simplex minimization resulted in a rate expression of

$$k_{11} = 1.54 \times 10^{13} \exp(-194.7 \text{ kJ mol}^{-1}/RT) \text{ s}^{-1}$$

for this reaction. The activation energy of 194.7 kJ mol<sup>-1</sup> is lower than that typically observed for hydrocarbon systems.<sup>26</sup> The presently reported activation energy compares favorably to that in the decomposition of 1,6-heptadiene reported initially by Eggers and Vitin<sup>27</sup> and extended to a wider temperature range by King.<sup>28</sup> The measured Arrhenius expression in the decomposition of 1,6-heptadiene was found to be<sup>27,28</sup>

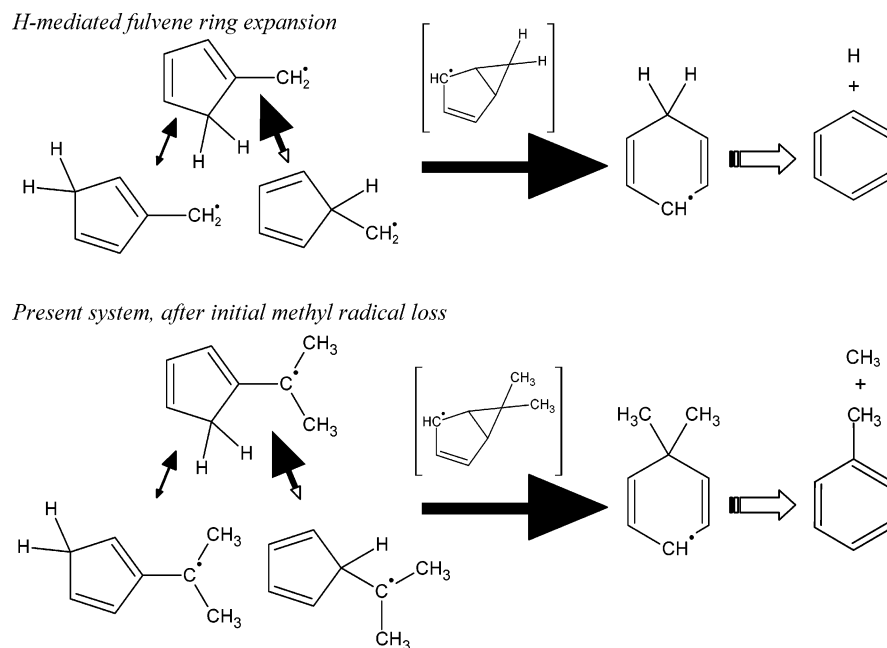
$$k = 2.0 \times 10^{11} \exp(-197 \text{ kJ mol}^{-1}/RT) \text{ s}^{-1}$$

As noted by Eggers and Vitin, resonance stabilization of the forming double bond within the cyclic six-membered transition state caused a decreased activation energy relative to that in 1-heptene. Similarly, in the present system, the double bond in the cyclopentadienyl moiety that is not directly participating in the reaction resonantly stabilizes the forming double bond in the transition state. As expected, the activation energy for the retro-ene reaction in 5-TBCP is similar to that for 1,6-heptadiene. The *A* factor is also higher for the retro-ene decomposition of 5-TBCP than for typical hydrocarbon retro-ene reactions.<sup>26</sup> This difference is due to the presence of nine labile hydrogen atoms in the *tert*-butyl moiety that react with two equivalent double bonds in the cyclopentadienyl ring.

The H-loss reactions shown in Scheme 6 are relatively minor channels, and no attempt to fit the final products was made. However, because these reactions have the effect of removing isopropyl-1-Cp and isopropyl-2-Cp from the system, we modeled the H-loss reactions from both species. The Arrhenius parameters from the reaction of isopropyl-1-Cp were allowed to float, and those of the isopropyl-2-Cp H-loss channel were fixed relative to them based on G3MP2B3 calculations as described above. These values are included in Table 3.

**Application to Fulvene Systems.** Although the present system is not expected to play a role in the sooting or PAH-forming reactions in the combustion of typical hydrocarbon fuels, it provides an experimentally convenient means to probe radical-assisted ring-expansion reactions that likely play a role in such systems. The mechanism proposed in Schemes 1–5 is analogous to that initially proposed by Melius et al. for the H-assisted ring expansion of fulvene to benzene.<sup>4</sup> In that mechanism, H adds to fulvene, producing 1-, 2-, and 5-(1,3-cyclopentadienyl)methyl radicals, which are analogous to the isopropyl-1-, -2-, and -5-Cp radicals here (Scheme 4). As is the case with isopropyl-5-Cp, the 5-(1,3-cyclopentadienyl)-methyl radicals are significantly higher in energy; however, ring expansion occurs only from that isomer. The ring expansion from the 5-(1,3-cyclopentadienyl)methyl radical has been predicted<sup>4</sup> to occur analogously to the reaction shown in Scheme 5, where the radical site reacts with one of the double bonds in the cyclopentadienyl ring, forming a three-centered intermediate species. The expansion of the five-membered ring then occurs by the opening of the three-centered moiety, followed by subsequent ejection of an H atom to form benzene.

Although the energetics of the reactions in the fulvene + H system differ from the present system (which is equivalent to a dimethylfulvene + H reaction), the general features of the mechanism appear to be identical. As illustrated in Figure 3, the formation of the six-membered product in the fulvene + H reaction is rate-limited by the formation of the 5-(1,3-cyclopentadienyl)methyl radical. Melius et al. calculated a barrier to isomerization of the 1 → 5 isomers of (1,3-cyclopentadienyl)-



**Figure 3.** Parallels between proposed mechanism for H-mediated fulvene expansion to form benzene and presently proposed mechanism. The areas of the solid arrowheads provide a pictorial representation of the reaction rates for each step. The areas of the hollow arrowheads have been scaled by 1000 $\times$ . The present experiment is not sensitive to the rate of the final step and is indicated with a stylized arrow that carries no information on the rate constant.

methyl radicals of 179 kJ mol<sup>-1</sup>, and Dubnikova and Lifshitz found an activation energy from QCISD(T)/cc-pVdz calculations of 176 kJ mol<sup>-1</sup> for the same reaction. A value of 148 kJ mol<sup>-1</sup> for the activation energy of the isopropyl-1-Cp  $\rightarrow$  isopropyl-5-Cp reaction was found to provide a good fit to our experimental product distributions. The predicted activation barriers for the two reactions are similar, and it is expected that the ring expansions occur along these similar pathways. In addition, Dubnikova and Lifshitz calculated Arrhenius parameters for the 5-(1,3-cyclopentadienyl)methyl radical conversion to cyclohexadienyl radical and found that the *A* factor was  $1.4 \times 10^{13}$  s<sup>-1</sup> and the activation energy was 72.8 kJ mol<sup>-1</sup>. At 1050 K, this yields a rate constant of  $3.3 \times 10^9$  s<sup>-1</sup>, which is substantially higher than the calculated  $1 \rightarrow 5$  isomerization rate constant in the (1,3-cyclopentadienyl)methyl species of  $1.3 \times 10^5$  s<sup>-1</sup> at the same temperature. The present mechanism includes this assumption and is consistent with the measured data. We conclude that the rate-limiting step in the H-assisted expansion of fulvene to benzene is the isomerization to form 5-(1,3-cyclopentadienyl)methyl radicals.

## Conclusion

Overall, the proposed mechanism for the decomposition of the isomers of *tert*-butyl cyclopentadiene is consistent with that proposed by Melius et al. for the H-assisted ring-opening reactions of fulvene. Previous studies of the pyrolysis of methyl-(1,3-cyclopentadienes) have been hampered by the requirement that large radical concentrations be present to allow bimolecular initiation of the ring-expansion reactions.<sup>6,7</sup> In the present study, the use of *t*-butyl-(1,3-cyclopentadiene) in lieu of methyl-(1,3-cyclopentadiene) produced radicals similar to those found in the H + fulvene ring-opening reactions (namely, the isopropyl-*n*-Cp radicals) without the need for bimolecular reactions. The use of a radical scavenger served both to eliminate chain process interference and to provide a means to further probe the mechanism by monitoring H-atom concentrations. We observed the expansion of the five-membered rings system to a six-membered aromatic ring system in a shock tube in the

temperature range of 1000–1100 K. We found that the ring-expansion reactions are rate-limited by the formation of isopropyl-5-Cp radicals, which subsequently undergo rapid ring expansion followed by loss of methyl radical to form toluene. This mechanism is fully consistent with previously proposed mechanisms for the H + fulvene reaction, in which the isomerization to form 5-(1,3-cyclopentadienyl)methyl radicals is the rate-limiting step in the formation of the six-membered ring.

**Supporting Information Available:** Results of the G3MP2B3 calculations, calculated thermochemical tables for the species shown in Table 5, and measured product concentrations as a function of temperature. This material is available free of charge via the Internet at <http://pubs.acs.org>.

## References and Notes

- (1) Richter, H.; Howard, J. B. *Prog. Energy Combust. Sci.* **2000**, *26*, 565–608.
- (2) Miller, J. A.; Klippenstein, S. J. *J. Phys. Chem. A* **2001**, *105*, 7254–7266.
- (3) Miller, J. A.; Klippenstein, S. J. *J. Phys. Chem. A* **2003**, *107*, 7783–7799.
- (4) Melius, C. F.; Colvin, M. E.; Marinov, N. M.; Pitz, W. J.; Senkan, S. M. *Proc. Combust. Inst.* **1996**, *26*, 685–692.
- (5) Dubnikova, F.; Lifshitz, A. *J. Phys. Chem. A* **2002**, *106*, 8173–8183.
- (6) Ikeda, E.; Tranter, R. S.; Kiefer, J. H.; Kern, R. D.; Singh, H. J.; Zhang, Q. *Proc. Combust. Inst.* **2000**, *28*, 1725–1732.
- (7) Lifshitz, A.; Tamburu, C.; Suslensky, A.; Dubnikova, F. *Proc. Combust. Inst.* **2005**, *30*, 1039–1047.
- (8) Certain commercial materials and equipment are identified in this paper in order to specify adequately the experimental procedure. In no case does such identification imply recommendation or endorsement by the National Institute of Standards and Technology, nor does it imply that the material or equipment is necessarily the best available for the purpose.
- (9) Tsang, W. In *Shock Waves in Chemistry*; Lifshitz, A., Ed.; Marcel Dekker: New York, 1981; pp 59–129.
- (10) Herzler, J.; Manion, J. A.; Tsang, W. *Int. J. Chem. Kinet.* **2001**, *33*, 755–767.
- (11) Benson, S. W.; O'Neal, H. E. *Kinetic Data on Gas-Phase Unimolecular Reactions*; National Standard Reference Data Series; National Bureau of Standards (United States): Washington, DC, 1970; Vol. 21, p 159.

- (12) Manion, J. A.; Tsang, W. *J. Phys. Chem.* **1996**, *100*, 7060–7065.
- (13) Tsang, W. *J. Phys. Chem. Ref. Data* **1990**, *19*, 1–68.
- (14) Radhakrishnan, K.; Hindmarsh, A. C. *Description and Use of LSODE, the Livermore Solver for Ordinary Differential Equations*; Report UCRL-ID-113855; Lawrence Livermore National Laboratory: Livermore, CA, 1993.
- (15) Jones, E.; Oliphant, T.; Peterson, P. *Scipy: Open Source Tools for Python*, 2001; available at <http://www.scipy.org>.
- (16) Press, W. H.; Flannery, B. P.; Teukolsky, S. A.; Vetterling, W. T. *Numerical Recipes in C: The Art of Scientific Computing*; Cambridge University Press: Cambridge, U.K., 1992; Chapter 10.
- (17) Tsang, W. *J. Chem. Phys.* **1966**, *44*, 4283–4295.
- (18) Roy, K.; Braun-Unkoff, M.; Frank, P.; Just, Th. *Int. J. Chem. Kinet.* **2001**, *33*, 821–833.
- (19) Roth, W. R. *Tetrahedron Lett.* **1964**, *17*, 1009–1013.
- (20) McLean, S.; Haynes, P. *Tetrahedron* **1965**, *21*, 2329–2342.
- (21) Bachrach, S. M. *J. Org. Chem.* **1993**, *58*, 5414–5421.
- (22) Baboul, A. G.; Curtiss, L. A.; Redfern, P. C.; Raghavachari, K. *J. Chem. Phys.* **1999**, *110*, 7650–7657.
- (23) Frisch, M. J.; Trucks, G. W.; Schlegel, H. B.; Scuseria, G. E.; Robb, M. A.; Cheeseman, J. R.; Montgomery, J. A., Jr.; Vreven, T.; Kudin, K. N.; Burant, J. C.; Millam, J. M.; Iyengar, S. S.; Tomasi, J.; Barone, V.; Mennucci, B.; Cossi, M.; Scalmani, G.; Rega, N.; Petersson, G. A.; Nakatsuji, H.; Hada, M.; Ehara, M.; Toyota, K.; Fukuda, R.; Hasegawa, J.; Ishida, M.; Nakajima, T.; Honda, Y.; Kitao, O.; Nakai, H.; Klene, M.; Li, X.; Knox, J. E.; Hratchian, H. P.; Cross, J. B.; Bakken, V.; Adamo, C.; Jaramillo, J.; Gomperts, R.; Stratmann, R. E.; Yazyev, O.; Austin, A. J.; Cammi, R.; Pomelli, C.; Ochterski, J. W.; Ayala, P. Y.; Morokuma, K.; Voth, G. A.; Salvador, P.; Dannenberg, J. J.; Zakrzewski, V. G.; Dapprich, S.; Daniels, A. D.; Strain, M. C.; Farkas, O.; Malick, D. K.; Rabuck, A. D.; Raghavachari, K.; Foresman, J. B.; Ortiz, J. V.; Cui, Q.; Baboul, A. G.; Clifford, S.; Cioslowski, J.; Stefanov, B. B.; Liu, G.; Liashenko, A.; Piskorz, P.; Komaromi, I.; Martin, R. L.; Fox, D. J.; Keith, T.; Al-Laham, M. A.; Peng, C. Y.; Nanayakkara, A.; Challacombe, M.; Gill, P. M. W.; Johnson, B.; Chen, W.; Wong, M. W.; Gonzalez, C.; Pople, J. A. *Gaussian 03*, revision C.02; Gaussian, Inc.: Wallingford, CT, 2004.
- (24) Tsang, W. A Pre-processor for the Generation of Chemical Kinetics Data for Simulations. Presented at the 39th AIAA Aerospace Sciences Meeting and Exhibit, Reno, NV, Jan 8–11, 2001; AIAA-2001-0359.
- (25) Tsang, W.; Bedanov, V.; Zachariah, M. R. *J. Phys. Chem.* **1996**, *100*, 4011–4018.
- (26) Tsang, W.; Lifshitz, A. In *Handbook of Shock Waves*; Ben-Dor, G., Igra, E., Elperin, T., Lifshitz, A., Eds.; Academic Press: San Diego, CA, 2001; Vol. 3, pp 107–210.
- (27) Eggers, K. W.; Vitins, P. *J. Am. Chem. Soc.* **1974**, *96*, 2714–2719.
- (28) King, K. D. *J. Phys. Chem.* **1980**, *84*, 2517–2521.